Journal of Thermal Analysis and Calorimetry, Vol. 72 (2003) 165–172

THERMAL CONDITIONS OF GROWTH AND THE NECKING EVOLUTION OF Si, GaSb AND GaAs
Glide phenomenon in the GaSb bowl*

*B. Štěpánek, J. Šesták**, J. J. Mareš and V. Šestáková*

Institute of Physics, Academy of Sciences of the Czech Republic, Cukrovarnická 10, 162 00 Prague, Czech Republic

Abstract

The configuration of thermal gradient is illustrated for various types of crucible rotation, which is important for the creation of dislocations, which decreases along the grown axis of crystal. A new mechanism for dislocation elimination during the growth is proposed to explain this phenomenon, which provides a good agreement with the experimental results. The concentration of etch pits rapidly decreased from the beginning to the end of the crystals and the dislocation densities in the middle portion of all investigated crystals were found less than 10^2 cm^{-2}. The shallow vertical temperature gradients and virtually flat solidification interface prevented thermal stress from their building up in the crystals. As a result, the dislocation formation had random distribution. Using good necking procedures and choosing an appropriately oriented starting crystal with the shoulder angle <38.94° (assuming growth in <111> direction) it is possible to produce almost dislocation-free crystals without resorting to additional doping normally employed to reduce dislocation formation.

Keywords: doping, gallium antimonide, low dislocation density, single crystal growth, thermal gradients

Introduction

The practical importance of semiconductor materials, such as Si, GaAs, GaSb, for electronics and photonics is, of course, for years beyond any doubt. An introduction of novel epitaxially grown quantum devices, containing low-dimensional subsystems [1] (e. g. quantum wells, quantum dots) as well as further sophistication of classical semiconductor devices (IC's, lasers, detectors) put, however, new heavy demands on substrate materials the quality of which is decisive also for the quality of end products. Typical requirements of the substrate wafers are extreme chemical purity, lattice perfection, and thermal and mechanical stability. Besides, for special uses (e.g. detectors for green house gases) it is necessary to grow also tailored single crystals with the special doping [2].

---

* Dedicated to the 80th birthday of Professor Vladimír Šatava, Ph.D., D.Sc., Emeritus Professor of the Institute of Chemical Technology in Prague, one of those who formed theoretical basis of thermal analysis and of material science of silicates.

** Author for correspondence: E-mail: sestak@fzu.cz

1388–6150/2003/ $ 20.00

Akadémiai Kiadó, Budapest

Gallium antimonide (GaSb) belongs to the group of III/V compounds. Single crystals of GaSb [3] are used as substrate material for the fabrication of long wavelength detectors and lasers ($\lambda \approx 1.5$ μm). High quality GaSb substrates are required for the growth of the (GaIn)(AsP) epitaxial layers used in optical communications. Quaternary systems, $Ga_{1-x}In_xAs_{1-y}Sb_y$ or $Ga_{1-x}Al_xAs_{1-y}Sb_y$ which are suitable for these wavelengths, can be lattice-matched to GaSb by differential contraction during the cooling process because the expansion coefficient values of the layer and substrate are very close [4].

Not less important are the studies allied to the system thermodynamics, related to the distribution of thermal and concentration gradients [5–7] as well as to the evaluation of phase equilibrium [7–10]. It is a continuation of our previous papers published in J. Thermal Anal. [7, 9, 10]. We extend it by our theoretical modelling of the overall gradient distribution created as a result of local thermal and concentration conditions, where the type of the externally applied crystal motion and crucible rotation become demonstrative, cf. Fig. 1.

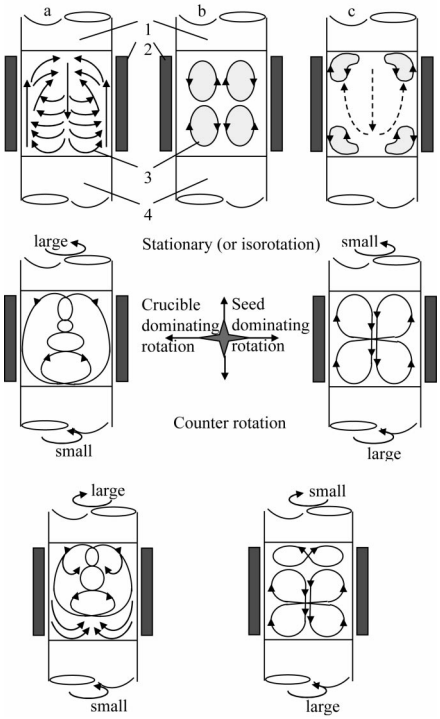

Fig. 1 Illustration of the gradients distribution (thick curves with arrows) shown for simplified arrangement of cylindrical melt container (crucible) heated from sides (shadow) with unmarked crystal growing seed. Upper line shows stationary disposition while middle line and bottom line portray iso-rotation and counter-rotation, respectively

Experimental

Studies of impurity type and concentration, free carrier concentration, types of conductivity and mainly dislocation density have to be carried out for GaSb single crystals. It is difficult to anticipate carrier concentration, especially with *n*-type conductivity, when preparing substrates. According to the literature [11–16], the concentration of residual acceptors in undoped GaSb single crystals is 1.0 to $2.7 \cdot 10^{17}$ atoms cm^{-3} *p*-type and, owing to the distribution effect of impurities, their concentration is changing in the direction of the crystal growth. To obtain a substrate with *n*-type conductivity and a low donor concentration level it is necessary to know to exact correlation between the concentration of impurities (deliberately added to the melt) and the consequent carrier concentration.

It is known that the dislocation density decreases in the direction of the crystal growth; this decrease is of the order of 10^2 to 10^4 cm^{-2} [17, 18]. Some authors [15, 17, 19] have found that the undoped crystals are relatively poor in quality. Doping of some elements reduces the formation of dislocations as a result of the higher thermal stress which are always inherent in the Czochralski technique (as manifested by most III–V compounds [20]). Using low temperature gradients in the furnace also decreases the possibility of dislocation formation and thus dislocation-free crystals can be grown.

The aim of our investigation was to study creation of dislocation and to find critical source causing multiplication of dislocations. For this study, Te-doped and undoped GaSb single crystals were grown using the Czochralski method without encapsulant and under low temperature gradient conditions along a solidification surface. The Czochralski apparatus technique without encapsulant was found to be very suitable for crystal growth (Fig. 2), and the standard distribution of temperature and concentration are shown in Fig. 3 completing thus the illustrative picture of the rotation consequences, cf. Fig. 1.

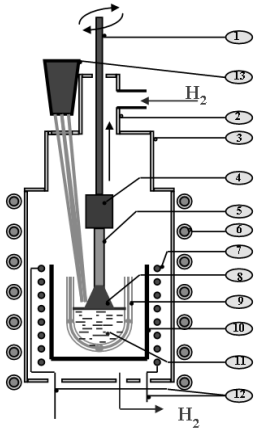

Fig. 2 Schematic diagram of the Czochralski apparatus for GaSb single crystal growth. 1 – sliding rod, 2 – top part of the apparatus, 3 – quartz tube, 4 – holder of the seed, 5 – seed, 6 – water cooling, 7 – molybdenum wire coils, 8 – GaSb single crystal, 9 – quartz crucible, 10 – graphite cylinder, 11 – melt of GaSb, 12 – power supplier, 13 – deuterium lamp

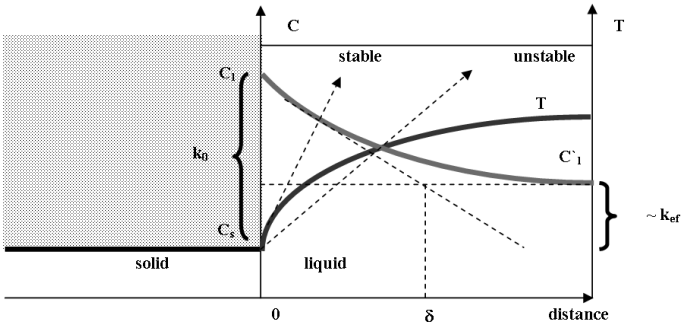

Fig. 3 The solid–liquid interface of the growing crystal illustrating the adhering surface layer, δ, with the concentration gradient, *C*, associated with the distribution coefficient, *k*. The rising curve shows the temperature profile, *T*, and the declining curve depicts the decrease concentration. The arrows separate the working conditions to regions of stable and metastable growth

In given crystals, we have found that the etch-pit densities (EPD) decreased with growth distance measured relatively to the seed. Such a behaviour had already read reported in the literature and various explanations had been proposed:

- according to Benz and Müller [21], dislocation pairs of opposite Burgers' vectors can annihilate one another;
- according to Yip and Wilcox [22], dislocations are eliminated by growing out of the crystal because they propagate normal to a solidification interface that is convex towards the liquid.
- However, none of these mechanisms can explain our results.
- annihilation works only when the dislocation densities are high (over 10^5 per cm^2 [23]);
- our solidification interfaces are almost flat and even slightly concave towards the liquid when growth begins; thus the Yip and Wilcox mechanism does not apply.

To explain our results, we supposed that the dislocations remained in the (111) dense planes of 'zinc-blende' structure (schematic positions of <111> planes are shown

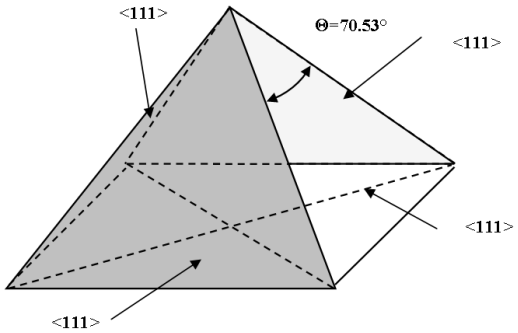

Fig. 4 Schematic position of <111> planes and their mutual angles

in Fig. 4), even up to temperatures close to the melting point. Inclined with respect to the [111] growth axis, they are gathered on the lateral surfaces during solidification.

If this were the single operating mechanism, we would get crystals absolutely free from dislocations. To take into account the remaining defects, we were led to consider that even below the CRSS (critical resolved shear stress) threshold (there is obviously no significant increase in dislocation density), residual glide can hamper elimination by forcing cross-slip of dislocations about to leave the crystals. Furthermore, direct creation by a Frank–Read mechanism cannot be ruled out, though it is certainly limited.

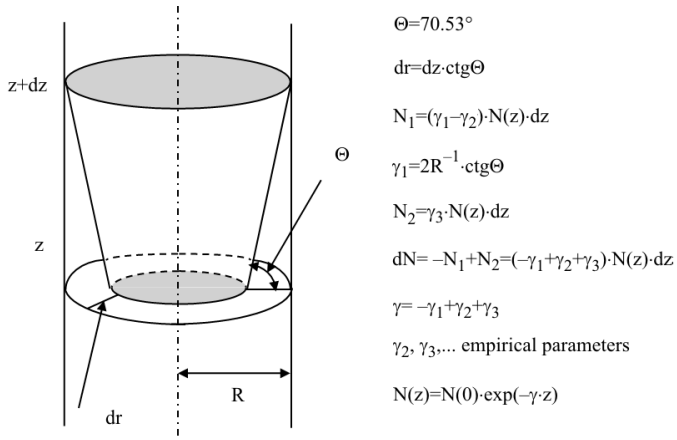

Fig. 5 Dislocation elimination on lateral surfaces during growth

Let us consider (Fig. 5) an element of crystal of height dz. Let Θ be the angle between the (111) growth plane and the other (111) planes (Θ=70.53°). The dislocations in the ring of width dr=dz cotΘ grow out when the interface moves from z to z+dz, unless they cross-slip and turn back to the inside of the crystal. The number of dislocations remaining between z and z+dz is

$$N_1 = (\gamma_1 - \gamma_2)\, N(z)\mathrm{d}z \tag{1}$$

where $N(z)$ is the number of dislocations at the height z. Supposing the etch-pits to be randomly distributed over the surface of the slice (an assumption we found to be valid for densities over 500 per cm^2), γ_1 dz simply represents the ratio of the surface of the ring to the total surface of the discuss of radius R; on the other hand, γ_2, is an empirical parameter depending on the linear density of defects that can cause cross-slip.

γ_1 can be easily calculated:

$$\gamma_1 \mathrm{d}z = \frac{2\pi R\,\mathrm{d}r}{\pi R^2} \quad \text{or} \quad \gamma_1 = \frac{2\cot\Theta}{R} \tag{2}$$

Since in our experiments R =0.5 cm, we find γ_1=1.4 cm^{-1}.

Let us consider that N_2 is the number of residual glide-induced dislocations at the origin; we will assume the equation of N_2=γ_3 $N(z)$ dz, where γ_3 is another empiri-

cal parameter depending on the linear density of defects that can cause pinning and multiplication of existing dislocations throughout the solidification.

A condition of balance of dislocations leads to

$$dN = -N_1 + N_2 = (-\gamma_1 + \gamma_2 + \gamma_3)\, N(z)\, dz \tag{3}$$

Assuming γ_2 and γ_3 to be independent of z (γ_1 is clearly independent of z since the dislocation distribution is uniform on a slice), the above equation can be easily integrated:

$$N(z) = N(0) \exp(-\gamma z) \tag{4}$$

where $\gamma = -\gamma_1 + \gamma_2 + \gamma_3$ and $N(0)$ is the dislocation density in the seed. Measurements done before and after crystallization proved that this value did not change during growth. The first experimental points are not exactly at the bottom end of the samples, due to some losses in the polishing procedure.

Linear regression on the experimental data was used to find the 'best fit' value of γ. It can be noticed that in spite of making a lot of simplifying approximations, the empirical equation fits well the experimental data.

Another interesting point is that the value of γ obtained with the best fit procedure (cca 1.1 cm^{-1}) is close to the value of γ_1 (1.4 cm^{-1}). This indicates that the elimination mechanism is by far the most important one, even though glide phenomena have also to be taken into account.

For crystals grown in the <111> direction we predicted that dislocations are eliminated during solidification on the lateral surfaces of the crystal owing to the glide phenomenon. We propose that this mechanism explains our results. In order to obtain a true correlation with experimental data, the starting angle between the <111> growth plane and the other <111> planes (70.53°) has to be equal 19.47°. If the starting angle between the shoulders of the crystal were below 38.94°, the dislocations would remain. Existence of such a mechanism was confirmed by studying our pre-

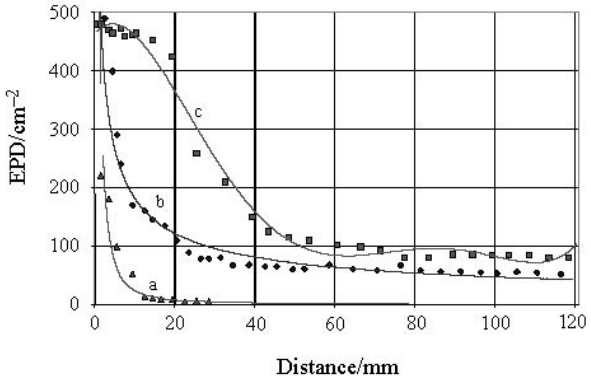

Fig. 6 Dislocation density longitudinal to the growth direction <111> of the GaSb single crystals. The curves show the dislocation profiles for different crystals shoulder initial angles. a – for an angle of 14.2°; b – 23.8° and c – first 15 mm at an angle of 46.8° and then 20 mm at an angle of 29°

pared GaSb crystals. We grew crystals with a different starting angle of crystal shoulders or we changed this angle during the growth.

The dislocation density (EPD) profiles of the crystals with different starting angles are shown in Fig. 6.

Crystals with a starting angle <38.94°showed decreasing EPD profiles; but in the case of the GaSb crystals (Fig. 6, curve (c)), where the starting angle was 46.8°, the dislocation density slowly increased. After reducing the neck angle to 29.0° the dislocation density started to reduce. In the centre of all crystals grown with a starting angle <38.94° the dislocation density decreased to a value of <10 cm^{-2}.

The same results were observed for Te-doped GaSb single crystals. If the starting angle was lower than 38.94° the dislocation density decreased so that it was possible to produce a dislocation-free area at the end of crystals. We grew Te-doped crystals with starting angles of about 24° and the dislocation density was measured using four Te-doped crystals with different concentration of tellurium. For each crystal was the dislocation density calculated from wafers taken from the central part of the crystal.

Conclusion

For the low thermal gradient configuration, which seems be most appropriate for the rotation set up where the crystal seed rotates fast and crucible slow (under counter-rotation, cf. Fig. 1), the number of dislocations decreases along the crystal. A new mechanism for dislocation elimination during growth is proposed to explain this phenomenon. The agreement with the experimental results is very good. The concentration of etch pits rapidly decreased from the beginning to the end of the crystals and the dislocation densities in the middle portion of all investigated crystals were $<10^2$ cm^{-2}. The shallow vertical temperature gradients and virtually flat solidification interface prevented thermal stress from building up in the crystals. As a result, the dislocation formation had random distribution. Therefore, Te doping was not found to influence EPD so there was no evidence of the existence of the so-called 'hardening effect'. Using good necking procedures and choosing a starting crystal shoulder angle <38.94° (assuming growth in <111> direction) it is possible to produce dislocation-free crystals without resorting to Te doping to reduce dislocation formation.

* * *

The author express thanks and gratitude to Grant Agency of the Academy of Sciences; particularly the projects No. A 4010101 and No. A 1010806 are especially acknowledged, as well as one, which is under the process of application at the Grant Agency of Czech Republic. The study was also done under the cooperation project MFM 'Research and modeling of systems and processes multiscalecharacter' No 230000009, carried out at the Institute of Interdisciplinary Studies, the West Bohemian University, Husova 17, CZ-30114 Pilsen, Czech Republic.

References

1 J. J. Mareš, J. Krištofik and P. Hubík, Phys. Rev. Lett., 82 (1999) 4699.
2 B. Štěpánek, V. Šestáková and J. Šesták, J. Electr. Eng., 50 (1999) 5.
3 V. Šestáková, B. Štěpánek and J. Šesták, J. Crystal Growth, 165 (1996) 159.
4 M. Astles, A. Hill, A. J. Williams, P. J. Wright and M. J. A. Young, J. Electron. Mater., 15 (1984) 41.
5 J. P. Czarnecki, N. Koga, V. Šestáková and J. Šesták, J. Thermal Anal., 38 (1992) 575.
6 V. Šestáková, chapter 'Crucible-free zone melting' in the book: 'Modern materials and technologies' (J. Šesták, Z. Strnad and A. Tříska, Eds), Academia, Prague 1993, pp. 115–130 (in Czech).
7 J. Šesták and B. Štěpánek (Eds) 'Thermodynamic applications in material science' as a special issue of J. Thermal Anal., Vol. 43, Akadémiai Kiadó, Budapest 1995.
8 J. Šesták, J. Leitner, H. Yokakawa and B. Štěpánek, Thermochim. Acta, 245 (1994) 189.
9 J. Šesták, B. Štěpánek, H. Yokakawa and V. Šestáková, J. Thermal Anal., 43 (1995) 389.
10 J. Šesták, B. Štěpánek and V. Šestáková, J. Therm. Anal. Cal., 56 (1999) 749.
11 D. T. J. Hurle, in P. Hartman (Ed.), Crystal Growth: An Introduction, North Holland, Amsterdam 1973, pp. 210–247.
12 S. Tohno and A. Katsui, J. Electrochem. Soc., 128 (1981) 1614.
13 Y. J. van der Meulen, J. Phys. Chem. Solids, 28 (1967) 25.
14 B. Cockayne, V. W. Steward, G. T. Brown, W. R. MacEwan, M. L. Young and S. J. Courtney, J. Crystal Growth, 58 (1982) 267.
15 W. A. Sunder, R. L. Barns, T. Y. Kometani, J. M. Parsey, Jr. and R. A. Laudise, J. Crystal Growth, 78 (1986) 9.
16 B. Štěpánek and V. Šestáková, Thermochim. Acta, 209 (1992) 285.
17 S. Kondo and S. Miyazawa, J. Crystal Growth, 56 (1982) 39.
18 J. P. Garandet, T. Duffar and J. J. Favier, J. Crystal Growth, 96 (1989) 888.
19 S. Miyazawa, S. Kondo and M. Naganuma, J. Crystal Growth, 49 (1980) 670.
20 A. S. Jordan, A. R. von Neida and R. Caruso, J. Crystal Growth, 76 (1986) 243.
21 K. W. Benz and G. Müller, J. Crystal Growth, 46 (1979) 35.
22 V. F. S. Yip and W. R. Wilcox, J. Crystal Growth, 36 (1976) 29.
23 C. F. Boucher, Jr., O. Ueda, T. Bryskiewicz, J. Lagowski and H. C. Gatos, J. Appl. Phys., 61 (1987) 3.